A Numerical Evaluation of J-Integral for a Center-Cracked Plate Subject to Biaxial Thermomechanical Load

T.R. Hsu, G.G. Chen, Z.L. Gong
University of Manitoba, Dept. of Mechanical Engineering, Winnipeg, Manitoba R3T 2N2, Canada

Abstract

This paper presents the finite element formulation and solution of the J-integral for center-cracked plates subject to simultaneous application of thermal and mechanical loads.

Numerical results indicates: (1) Both temperature field and bi-axial loadings have significant effects on the J-integral evaluations; (2) The effect of the bi-axial loading factor is more significant with thernal effect; (3) J-values depend on the sequence of the thermal and mechanical load.

1. Introduction

The J-integral concept has been widely used by researchers to characterize cracks in ductile materials ever since its inception in 1968 [1]. The main reason for its popularity is that it can be readily evaluated by a contour integration along a conveniently selected path which encloses the tip of the crack. This path usually encompasses the region in which the elastic-plastic stress and strain fields can be determined with sufficient accuracy, and thus reduce the effect on the result by the overwhelming dominance of the steep stress and strain fields at the vicinity of the crack tip.

Despite the many meritorious aspects of the J-integral in dealing with the elasto-plastic fracture problems, several fundamental questions remain outstanding. Most formulations on the J-integral are based on the Mode I (opening mode) fracture with the load applied normal to a through crack. Little information is available about the effect of the bi-axial loadings on the J-integrals. The bi-axially loading conditions are common in the pipelines and thin wall pressure vessels. The effect of thermal load in the form of a temperature field on the J evaluation is another aspect which has not been extensively investigated.

The present study deals with a numerical investigation on the J-integral for a center-cracked plate subject to distributed mechanical loading, σ in the direction normal to the crack and $K\sigma$ along the line crack. The load ratio K varied between -2.0 to +2.0. The case of K = +2.0 may simulate a case of a circumferential through crack in a thin wall pipe whereas K = 0.5 assimilates a longitudinal through crack in the pipe.

2. Finite Element Formulation

Following the derivations presented in [2, 3], the expression for the J-integral with the presence of thermal strains may be shown as follows:

$$J = \int_\Gamma (W dx_2 - t_i \frac{\partial u_i}{\partial x_1}) dS + \int_{A_o} \alpha \sigma_{ii} \frac{\partial T}{\partial x_1} dA \quad (1)$$

(sum over i = 1, 2, 3)

where t_i and u_i are the respective surface traction normal to the contour and the displacement components in the elements on the contour; α, T and σ_{ii} are the linear thermal expansion coefficient, above-reference temperature and normal stress components in the elements on and within the contour for the integration. The physical meaning of the coordinates x_1, x_2, the contour Γ and the enclosed area A_o as well as dS and dA have been illustrated in Fig. 1.

It is obvious that Eq.(1) can be shown to be identical to the usual form of J-integral when the temperature gradients in the second term vanishes.

The strain energy density W in the above expression is defined as:

$$W = \int_o^{\varepsilon_{ij}} \sigma_{ij} \, d\varepsilon_{ij} \quad (2)$$

where the combined thermomechanical strain components may be computed from:

$$\varepsilon_{ij} = \varepsilon_{ij}^m - \alpha T \delta_{ij}$$

in which ε_{ij}^m are the strain components due to mechanical loads only and δ_{ij} is the Kronecker delta.

The discretized form of Eq.(1) suitable for the finite element analysis can be shown as follows [2]:

$$J = \sum_{m=1}^{M} \{W_m \Delta y_m - [t_m^x (\frac{\Delta u}{\Delta x})_m + t_m^y (\frac{\Delta v}{\Delta x})_m] \Delta S_m\}$$
$$+ \alpha \sum_{n=1}^{N} (\sigma_{xx,n} + \sigma_{yy,n} + \sigma_{zz,n}) (\frac{\Delta T}{\Delta x})_n A_n \quad (3)$$

in which the subscripts m and n denote the quantities associated with the elements on the contour Γ and those elements on and within the contour.

3. Numerical Illustration

The case of a center-cracked long strip was considered with the geometry and dimensions described in Fig. 2. Only one quarter of the plate was included in the finite element model due to symmetry. Uniform tensile or compressive loads (σ_1 and σ_2) were applied at the edges of the plate. Variation of σ_1 and σ_2 may be indicated by the load factor K defined as:

$$K = \sigma_1 / \sigma_2$$

A negative K will mean a $-\sigma_1$ only in the subsequent presentation.

A temperature variation in the x_1 direction was assumed. The function used in the present illustration is:

$$T(x) = \Delta T (\frac{x}{w})^2 \quad (4)$$

which can induce an apparent thermoelastic stress field of

$$\sigma_T(x) = E \alpha \Delta T [\frac{1}{3} - (\frac{x}{w})^2] \quad (5)$$

in an uncracked plate [3]. The term ΔT denotes the temperature difference between the edge and the center of the plate.

An algorithm following Eq.(3) was incorporated in a thermomechanical finite element stress analysis code TEPSA [2] with the following temperature-independent material properties: Young's modulus E = 1400 GPa, plastic tangent modulus, E' = 700 MPa, Poisson's ratio $\nu = 0.3$, initial yield strength, $\sigma_y = 145$ MPa, $\alpha = 10 \times 10^{-6}/^{o}F$.

A total of 3 distinct contours, Γ_1, Γ_2 and Γ_3 were chosen for the computation as shown in Fig. 3.

A temperature field following Eq.(4) with ΔT vary according to Fig. 4 was introduced in the plate. Also shown in this figure is the normalized mechanical loads represented by σ_2/σ_y curve.

Figs. 5 and 6 show the J values in the plate at various levels of thermomechanical loadings and bi-axial loading factors whereas the results from pure mechanical loading cases are illustrated in Fig. 7. Fig. 8 shows the plastic zone size versus K factors. The shapes of these plastic zones for both thermomechanical and mechanical loading cases are depicted in Fig. 9.

One unique response of solid to the thermomechanical loading is the dependence on the loading sequence [2]. It is interesting to note that the same dependence also applies to the J evaluation. As all results obtained in the previous cases were related to the mechanical loading of a "preheated" plate (Fig. 4), a reversed sequence of load application was assumed in this case as described in Fig. 10. Significant deviation of J values can be observed even at identical final states as illustrated in Fig. 11.

4. Discussion of Numerical Results

Comparison of results obtained by the present finite element analysis and those by the analytical method was only possible for the case of uniaxial loading with K = 0. The equivalent J value under a global thermoelastic loading condition can be expressed to be:

$$J = E\alpha^2 \Delta T^2 \pi a[\frac{1}{3} - \frac{1}{2}(\frac{a}{w})^2]^2 + \frac{\sigma_2^2 \pi a}{E} \qquad (6)$$

Good agreement of results by these two methods was obtained as can be seen from Table 1.

Table 1 Comparison of J Parameters by F.E. and Analytical Methods

Temperature Difference ΔT, (^oF)	Mechanical Load σ_2/σ_y	J (KPa-mm)	
		F.E. Method	Analytical Method (Eq.(6))
66.56	0	50.12	50.23
76.80	0	67.00	66.88
76.80	0.05	98.71	97.91

The effect of bi-axial loading factor K on the J-integral is significant as can be observed in Figs. 5 and 6. The smallest value of J occured at K=1. The J values increase with K>1 and decrease rapidly as K becomes less than 1. The rates of variations accelerate with negative K values. The effect of K on J-integral apparently is more pronounced in the cases involving thermal effect than that on isothermal conditions. The latter cases have been described by Liebowitz et al [4]. A comparison of these results is available in Fig. 8 in which the dotted curve was translated from [4] by assuming a proportional ordinates used in the same reference.

Another significant effect on the J-integral evaluation with the presence of temperature field is the selection of paths for the contour integration. Excessive temperature variations and loadings in the cracked plate can invalidate the path-independent nature of the J-integral [2]. However, in the present case of K=0.5, the maximum deviation of the J values obtained by Γ_1 and Γ_2 depicted in Fig. 3 was only 2.4% whereas this deviation between values by Γ_1 and Γ_3 was at a much higher value of 22.7%. This inconsistency was attributed by the fact that Γ_3, being the smallest and closest to the crack tip, it contained an overwhelming portion of the material with very steep stress and strain gradients. Yet the finite mesh sizes, the "constant strain" element algorithm and the small strain elastic-plasticity theory on which the TEPSA code was constructed made accurate computation of key quantities involved in the J-integral virtually impossible in this region.

Finally, it is interesting to notice that J values are sensitive to the sequence of thermal and mechanical loadings. Noticeable deviations can be observed on the J values as illustrated in Fig. 11.

References

[1] Rice, J.R., "A Path Independent Integral and the Approximate Analysis of Strain Concentration by Notches and Cracks", Journal of Applied Mechanics A.S.M.E. Trans, 35 (2), 1968, pp.379-386.

[2] Hsu, T.R., "The Finite Element Method in Thermomechanics", Chapter 7: Thermofracture Mechanics, George Allen & Unwin (Publishers) Ltd.

[3] Ainsworth, R.A., Neal, B.K. and Hellen, T.K., "Fracture Behaviour in the Presence of Thermal Strains", Proc. of Conf. on tolerance of flaws in pressurized components, Institute of Mechanical Engineering, May 1978, pp.171-178.

[4] Liebowitz, H., Lee, J.D. and Eftis, J., "Bi-axial Load Effects in Fracture Mechanics", Engineering Fracture Mechanics, Vol. 10, 1978, pp.315-335.

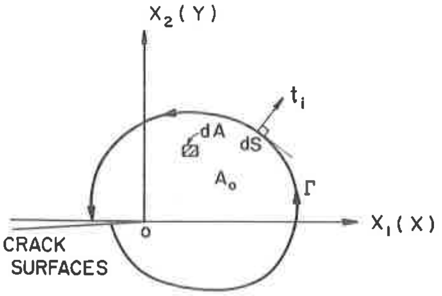

Fig. 1 Contour for J-Integral

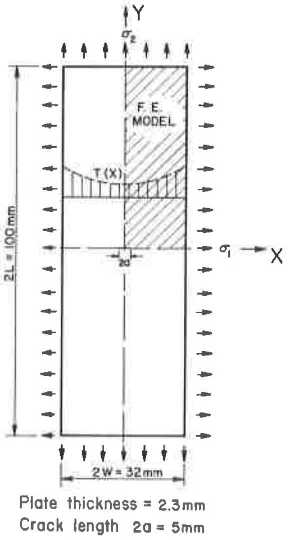

Fig. 2 Geometry and Finite Element Idealization of a Center-Cracked Plate with a Temperature Field

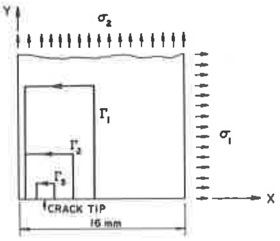

Fig. 3 Selected Contours for J Evaluations

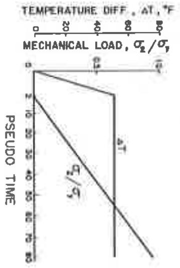

Fig. 4 Loading History on a Preheated Plate

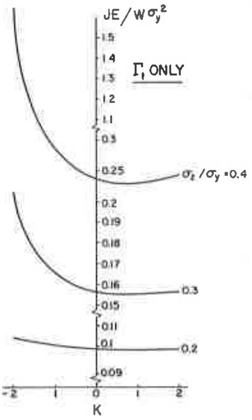

Fig. 5 Variation J vs K Factors

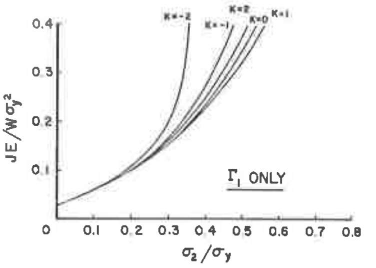

Fig. 6 Variation of J vs Loads with a Temperature Field

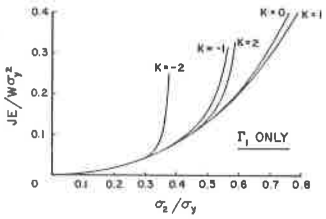

Fig. 7 Variation of J vs Loads in Isothermal Condition

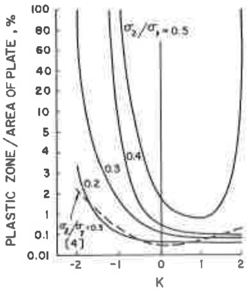

Fig. 8 Variation of Plastic Zone Size vs K Factors

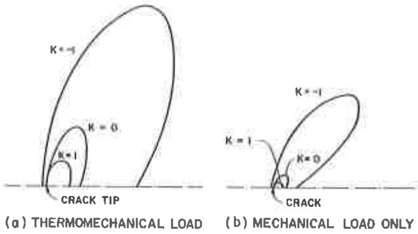

Fig. 9 Shapes of Plastic Zone at $\sigma_2/\sigma_y = 0.5$

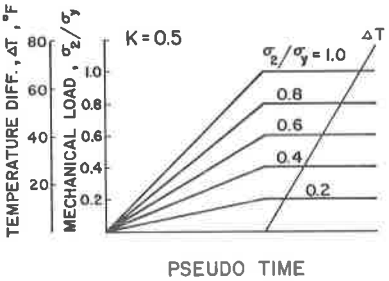

Fig. 10 Reversed Thermomechanical Loading History

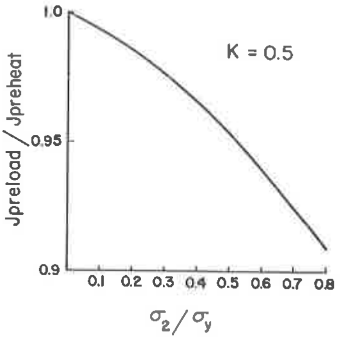

Fig. 11 Comparison of J Values with Reversed Loading Histories